frontiers in Earth Science

ORIGINAL RESEARCH
published: 02 March 2022
doi: 10.3389/feart.2022.730023

# The Volcano-Tectonics of the Northern Sector of Ischia Island Caldera (Southern Italy): Resurgence, Subsidence and Earthquakes

*Stefano Carlino*[1]*, *Alessandro Sbrana*[2], *Nicola Alessandro Pino*[1], *Paola Marianelli*[2], *Giuseppe Pasquini*[2], *Prospero De Martino*[1] and *Vincenzo De Novellis*[1,3]

[1]Istituto Nazionale di Geofisica e Vulcanologia, Sezione di Napoli—Osservatorio Vesuviano, Naples, Italy, [2]Earth Science Department, Università degli Studi di Pisa, Pisa, Italy, [3]Consiglio Nazionale delle Ricerche, Istituto per il Rilevamento Elettromagnetico dell'Ambiente, Naples, Italy

OPEN ACCESS

**Edited by:**
Luis E. Lara,
Servicio Nacional de Geología y Minería de Chile (SERNAGEOMIN), Chile

**Reviewed by:**
Micol Todesco,
Istituto Nazionale di Geofisica e Vulcanologia (INGV), Italy
Abdelsalam Salem Elshaafi,
University of Benghazi, Libya
Kyriaki Drymoni,
University of Milano-Bicocca, Italy

***Correspondence:**
Stefano Carlino
stefano.carlino@ingv.it

**Specialty section:**
This article was submitted to Volcanology, a section of the journal Frontiers in Earth Science

**Received:** 24 June 2021
**Accepted:** 21 January 2022
**Published:** 02 March 2022

**Citation:**
Carlino S, Sbrana A, Pino NA, Marianelli P, Pasquini G, De Martino P and De Novellis V (2022) The Volcano-Tectonics of the Northern Sector of Ischia Island Caldera (Southern Italy): Resurgence, Subsidence and Earthquakes. Front. Earth Sci. 10:730023. doi: 10.3389/feart.2022.730023

The island of Ischia, an active volcanic field emerging in the western sector of the Gulf of Naples (Southern Italy), represents an archetypal case of caldera that underwent a very large resurgence related to the intrusion of a shallow magma body. The resurgence culminated with the formation of a structural high in the central sector of the island, i.e., the Mt. Epomeo block. This is bordered by a system of faults along which volcanic activity occurred up to 1302 A.D., and damaging earthquakes were generated in historical and recent time. The seismicity is located prevalently in the northern sector of the island and appears to be correlated with the most recent phase (<5 ka) of ground movement (subsidence), although the mechanism of earthquakes' generation is still debated. By jointly analyzing offshore and onshore data (seismic profile and stratigraphy wells, respectively) and new petrological and geochemical data related to the most recent phase of volcano-tectonic activity, we develop a geological and structural layout of the northern sector of the island. In particular, we identify the seismogenic fault associated with the historical and recent destructive earthquakes of Ischia. This fault formed in the northern sector of the island during the final stage of the resurgence. We also propose a conceptual volcano-tectonic model of the northern sector of the Ischia Island, depicting the displacement of the fault zones in the off-shore area and the possible mechanism of stress loading and release in the on-shore zone, which is mainly driven by the subsidence of the Mt. Epomeo block. Our results are crucial for evaluating the dynamics of the seismogenic structures in the framework of the general subsidence of the island, as well as the related seismic hazard.

**Keywords: Ischia island, caldera resurgence, subsidence, earthquakes, faults, horst-graben**

## INTRODUCTION

Caldera long-term resurgence and subsidence represent primary processes that are generally associated alternatively to renewal of magma activity and following drainage/degassing or to fluid pressurization and depressurization (Marsh, 1984; Hurwitz et al., 2007; Kennedy et al., 2008). Resurgence sometimes culminates with an eruption, while subsidence is generally associated to low volcanic hazard and lower seismic activity (Acocella et al., 2015, and

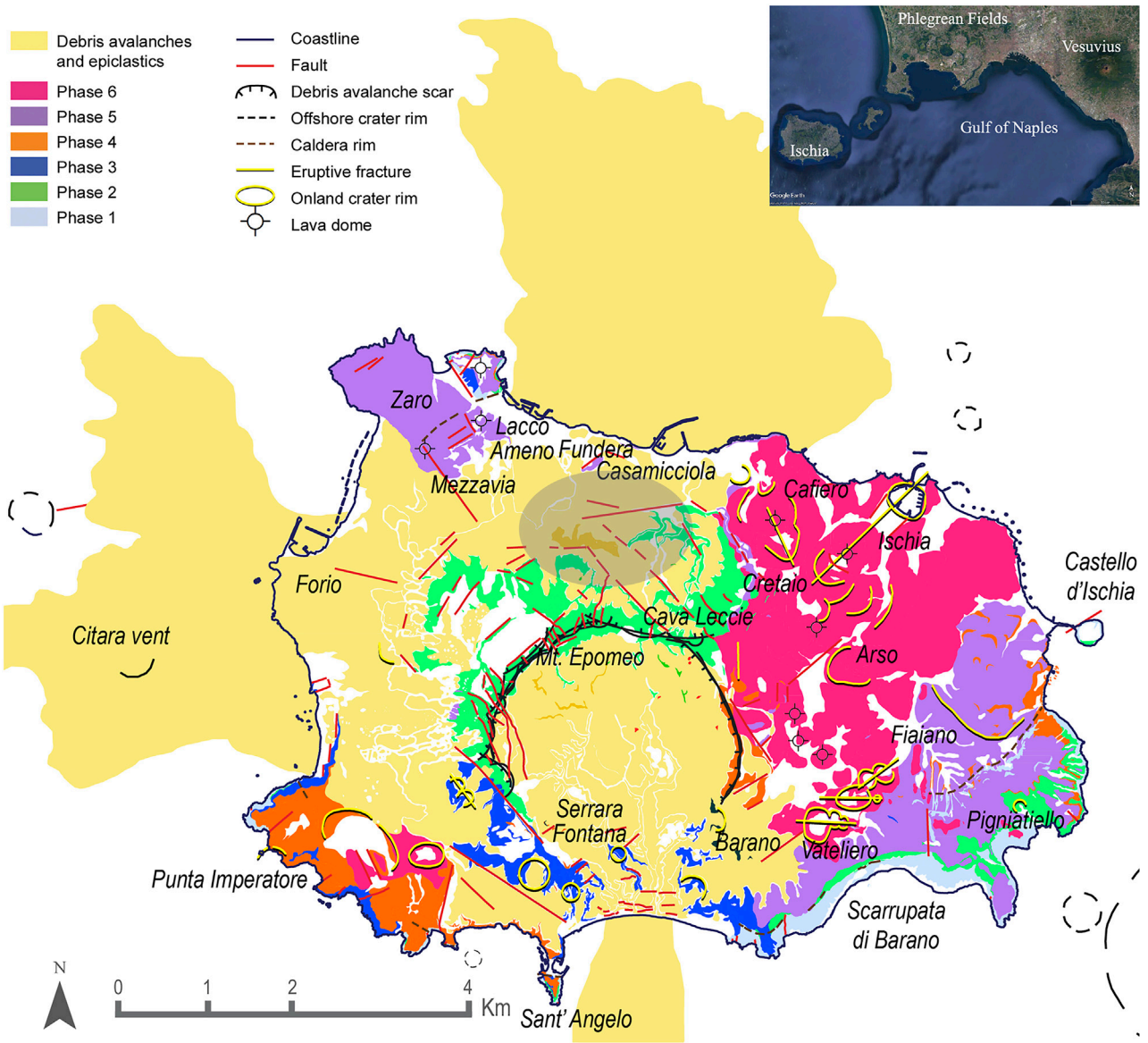


**FIGURE 1 |** Volcanological phases of Ischia volcanic field (Sbrana et al., 2018, modified). The gray shaded area is the zone affected by highest damage of historical and recent earthquakes in the island.

references therein). The general model of caldera resurgence is associated with magma intrusion in the shallow crust (after a caldera collapse), which perturbs the shallow aquifers generating large hot fluids advection (i.e., the geothermal system) and stressing the above crust, thus, producing bending, faulting, volcanic activity, and earthquakes (Cole et al., 2005; Kennedy et al., 2012; Branney and Acocella, 2015; Galetto et al., 2017). In this framework, the volcanically active island of Ischia (located in the Gulf of Naples, **Figure 1**) represents a very interesting case study of resurgent/subsiding caldera, as 1) it was characterized by unusual very large resurgence of about 1,000 m, from a time comprised between 56 and 33 to about 5 ka (Vezzoli 1988; Sbrana et al., 2009); 2) recurrent damaging earthquakes occurred in historical and recent times, during a phase of volcanic quiescence and subsidence (Sbrana et al., 2009; Carlino, 2012, 2021; De Novellis et al., 2018). In fact, after the last volcanic activity at Ischia, which occurred in 1302 A.D., a number of earthquakes generating heavy damage and fatalities (e.g., 1828, 1881, 1883) hit the northern sector of the island, in the area of Casamicciola Terme (**Table 1**; Cubellis and Luongo, 1998; Selva et al., 2021).

The most devastating event was in 1883, which caused more than 2,300 victims and the whole destruction of the town of Casamicciola Terme (Carlino et al., 2010; Carlino et al., 2021). In spite of their inferred relatively low magnitude (**Table 1**), the high damaging level of these events has been mainly ascribed to the

**TABLE 1 |** Historical seismicity in the island of Ischia as reported by Cubellis and Luongo, 1998.

| Year | Epicentral area | Epicentral intensity MCS | Magnitude | Damages |
|---|---|---|---|---|
| 1,228 | Casamicciola | IX–X* | — | 700 deaths, large landslide from Mt. Epomeo |
| 1,275 | Northern sector | VIII–IX (VIII–IX)< | (4.0) | Damages |
| 1,302 | Eastern area | VIII | — | Many buildings collapse |
| 1,557 | Southeast area | VII–VIII (VI–VII) | (3.5) | Collapse of the Parish Church |
| 1762 | Casamicciola | VII (VI–VII | (3.5) | Damage to houses in Casamicciola |
| 1767 | Eastern area | VII–VIII (VI–VII) | (3.5) | Collapse of Rotaro's Church |
| 1769 | Casamicciola | VIII | — | 7 deaths, serious damage in the upper part of Casamicciola |
| 1828 | Casamicciola | VIII–IX (VIII–IX) | (4.0) | 28 deaths, 50 injured, serious damage and collapses in the upper part of Casamicciola |
| 1841 | Casamicciola | VII (V–VI) | (3.3) | Cracks in the buildings |
| 1863 | Casamicciola | VII (VI–VII) | (4.9) | Collapse of dry walls, small landslides from Mt. Epomeo |
| 1867 | Casamicciola | VI–VII (IV–V) | (3.0) | Buildings damaged at Casamicciola |
| 1881 | Casamicciola | IX (IX) | (4.1) | 129 deaths, many injured, many collapsed buildings at Casamicciola and Lacco Ameno |
| 1883 | Casamicciola | XI (IX–X) | 4.6–5.2 (4.3) | 2,333 deaths, 762 injured, many collapsed at Casamicciola, Lacco Ameno and Forio |

*Note. Epicentral intensity and magnitude values from CPTI15 (Rovida et al., 2019) have been added in parentheses.*

shallowness of the seismogenic source, enclosed in the upper 1 km of depth (Cubellis and Luongo 1998; Carlino et al., 2010; De Novellis et al., 2018; Carlino et al., 2021). This latter feature has also been observed during the last $M_W$ = 3.9, 2017, earthquake that hit again the northern sector of the island, after 134 years of almost complete seismic silence, producing victims and damage. The W-E striking fault associated with this last event is located at the border of a system of subvertical faults that were formed during the resurgence of the central part of the island, for the volumetric growth of a shallow magma body, and, thus, are not related to the ring–fault system formed during the caldera collapse (Cubellis and Luongo, 1998; Acocella and Funiciello, 1999; Carlino et al., 2006; Sbrana et al., 2009; Carlino, 2012; Paoletti et al., 2013; Sbrana et al., 2018). The W-E seismogenic structure has been active at least during the last three centuries, likely during a phase of subsidence of the island (Carlino et al., 2021).

The mechanism leading to the earthquakes of the northern sector of the island, as well as the geometry and location of the source of the last event in 2017, have been recently interpreted by various authors, supporting different scenarios (Braun et al., 2018; De Novellis et al., 2018, 2019; Nappi et al., 2018; Calderoni et al., 2019; Trasatti et al., 2019). Also, the geometry of the faults active during the resurgence has been reported by various authors, based on geological data, and leading to different settings (Vezzoli, 1988; Orsi et al., 1991; Acocella and Funiciello, 1999; Sbrana et al., 2018). Inward and outward dipping fault systems are both invoked in the Mt. Epomeo resurgent processes. However, Carlino et al. (2021) recently showed that the historical and recent earthquakes of the island, in particular the 1881, 1883, and 2017 events, are generated by a single fault located at the northern base of the Mt. Epomeo.

A further in-depth analysis of the geological and tectonic features of the island is essential to: 1) better investigate the dynamics of the resurgence and the configuration of related faults; 2) recognize the seismogenic source and its relation with the past and ongoing island dynamic. This is an important goal, given the high volcanic and seismic risk of the area (Selva et al., 2019).

Thus, aiming to obtain a reference geological outline of both the uplifted structure and the seismogenic fault formed during the Mt. Epomeo resurgence, we have analyzed and interpreted geological and geophysical data relative to the northern area of the island. In particular, we jointly interpreted an N-S offshore seismic profile and onshore data related to the stratigraphic information obtained from boreholes, and used new petrological and geochemical data of the most recent phase of volcanic activity to understand its relation with the volcano tectonics. Finally, we focused on the seismogenic structure mentioned above, interpreting its origin and activity in the light of the data acquired and in the framework of the ongoing subsidence.

## GEOLOGICAL FRAMEWORK

The island of Ischia represents the emergent part of a much larger volcanic field, which develops predominantly in an east-west direction at the western end of the Gulf of Naples (Vezzoli. 1988; Sbrana et al., 2018) (**Figure 1**). It covers 46 $km^2$ mainly consisting of rocks that are derived from a number of explosive and effusive eruptions dating back to about 150 ka (Vezzoli. 1988). A shallow and very high-temperature geothermal system is developed on the island, with maximum geothermal gradients recorded in boreholes in the western and southern sectors (>180°C $km^{-1}$) (Sbrana et al., 2009; Carlino, 2018). The activity of the island has been divided into six main phases, summarized in **Table 2** (Sbrana et al., 2018). Several paroxistic plinian-to-ignimbritic eruptions (e.g., Pignatiello and Mt. Epomeo Green Tuff formations and phase 2 in Sbrana et al., (2018) induced a caldera collapse of about 60–56 ka. A subsequent stasis of volcanism with erosion phase and marine sedimentation partially filled the Ischia caldera depression. The starting of the resurgence occurred between the 56 ka caldera collapse and its refilling with sediments and epiclastics (phase 3 of Sbrana et al., 2018) and the observed sealing of the SW fault of the Mount Epomeo resurgent block by means of the yellow tuffs erupted by the Serrara Fontana vent aged to 33 ka. In fact, the yellow tuffs mantle unconformably the vertical fault plane,

**TABLE 2 |** Volcanic activity phases of Ischia (after Sbrana et al., 2018).

| Phase | Age | Description |
|---|---|---|
| Phase 1 | >150–73 ka | Ischia volcanic field building |
| Phase 2 | 60–56 ka | Caldera forming and filling |
| Phase 3 | 56?–33 ka | Post caldera activity—starting Mt. Epomeo block resurgence |
| Phase 4 | 29–13 ka | Post caldera activity—renewal of volcanic field activity |
| Phase 5 | 10–5 ka | New phase of caldera resurgence—Mt Epomeo uplift renewal |
| Phase 6 | 3.7 ka–1302 A.D. | Historical phase |

indicating that the Serrara vent, located along the SW fault of the resurgent block, opened (33 ka) when the resurgent block was largely uplifted. The outcrop where the described geometry of overlapping of yellow tuffs covering the fault plane of the resurgent block is at present times at about 600 m of elevation. Resurgence continued afterward, although geological evidence of its occurrence have been found until around 8–5 ka (Sbrana et al., 2011). This is accompanied by the activation of volcanism in the north (Zaro complex, Fundera, Casamicciola, Puzzillo volcanoes) and east sectors of the caldera and culminates with destabilization of the argillified tuffs of the resurgent block. The onset of the two main volcanic phases (4 and 5), starting, respectively, 29 and 10 ka, has been marked by decreased Sr and Nd isotope ratios, which indicate the arrival of new magma from a deeper feeding zone (Civetta et al., 1991). These two phases and the last one as well, have been characterized by the occurrence of small-to-moderate explosive eruptions and lava flows (Brown et al., 2008; Sbrana et al., 2018). The second main phase of resurgence (phases 5 and 6, **Table 2**) (Sbrana et al., 2009, 2018) involved the central part of the island (i.e., the Mt. Epomeo block) up to the Grande Sentinella (**Figure 2**), and was associated with different inputs of magma at shallow depths, after the phase 4, producing volcanic deposits of significantly different compositions with respect to those of the previous eruptions (Civetta et al., 1991).

The renewal of the resurgence, between the phase 5 and 6, generated the gravitational instability of the flank of the resurgent structure (Mt. Epomeo), triggering sector collapses and consequent emplacement of debris avalanches along the northern, western, and southern sectors of the island (De Alteriis et al., 2010). The main structure of Mt. Epomeo emerges, nowadays, as an approximately $\sim 3 \times 3$-km$^2$ block, 787 m high (a.s.l.), bordered by a system of faults mainly oriented NW-SE, E-W, and N-S (Sbrana et al., 2009, 2018; Vezzoli et al., 2009; de Vita et al., 2010; Carlino, 2012). The outer faults, which limited the resurgent area (ring-faults), have been associated to caldera collapse, while the faults bordering the central block of Mt. Epomeo were formed during the resurgence (Acocella and Funiciello, 1999; Sbrana et al., 2018). In general, the formation of inward-dipping ring–faults or almost vertical faults is favored in the extensional zones, as is the case of Ischia Island (Holohan et al., 2005). Subvertical faults with slight inward or outward dip have been also observed around the resurgent block (Vezzoli, 1988; Acocella and Funiciello, 1999; Sbrana et al., 2018). The seismicity in the last three centuries is located along the northern rim of the resurgent block (**Figure 1**).

# DATA AND METHODS

## Onshore and Offshore Geological Data

The volcano-tectonic structural framework obtained in this study is derived from the combined interpretation of several data collected in the CARG project[1] (Servizio Geologico d'Italia, 2018, Geological map of Italy, F464 Isola d'Ischia, in a scale of 1:25,000, ISPRA; Carta Geologica della Regione Campania, scala 1:10,000, Foglio 464 Isola di Ischia, Note Illustrative, Regione Campania, Assessorato Difesa del Suolo. LAC Firenze; Sbrana et al., 2011), including on-land (subsurface geology reconstruction using thermal water borehole stratigraphies) and offshore information (bathymetry and seismic line acquired in CARG project in correspondence of the Lacco Ameno debris avalanche and reinterpreted in this paper) (**Figures 2** and **3**).

In particular, the stratigraphies used in this work (**Figure 3**) were derived from the water wells drilled for thermal use for hotels and spa-wellness center in the north sector of the island.

The offshore area is investigated using seismic line 21 (**Figure 4**), acquired in 2005 during geophysical CARG surveys, finalized to the geological and volcanological reconstruction of the marine areas of this active insular volcanic field (Sbrana et al., 2011).

High-resolution sparker seismic surveys were performed by Parthenope University staff by means of a single-channel reflection seismic system composed by the energizing one (EG&G Trigger Capacitor Bank mod. 231 and power supply mod. 232), the firing or seismic source (SAM96 sparker, at 96 electrodes), and the measuring receiver. The frequency range of the signal extends from 100 to 3,000 Hz, and the sampling rate is 12,000 samples per second. The measuring apparatus was composed of a hydrophonic chain, an amplifier, an anti-aliasing filter with a bandwidth from 150 to 3,000 Hz and by the D-Seismic acquisition system. The maximum vertical resolution is about 0.25 m, while the horizontal is about 3 m. Depths are expressed in milliseconds (two-way travel time) and converted in meters (for the calculation of the thicknesses of the various seismic units) considering the conventional speed of acoustic waves in water equal to 1,500 m/s. Multibeam surveys were carried out from the coastline to the depth of −200 m, in order to obtain detailed bathymetric map of the study area (Passaro et al., 2016). The positioning of the boat was detected with an Omnistar DGPS system with an error of about 1 m. The geophysical and geological interpretation of the high-resolution line is based on the good knowledge of the on-land geology and volcanology. This allows the team to perform an integrated interpretation of the main volcanic units on the island and of the seismic units, interpreted in terms of seismic facies and

[1]https://www.isprambiente.gov.it/it/progetti/cartella-progetti-in-corso/suolo-e-territorio-1/progetto-carg-cartografia-geologica-e-geotematica/index.

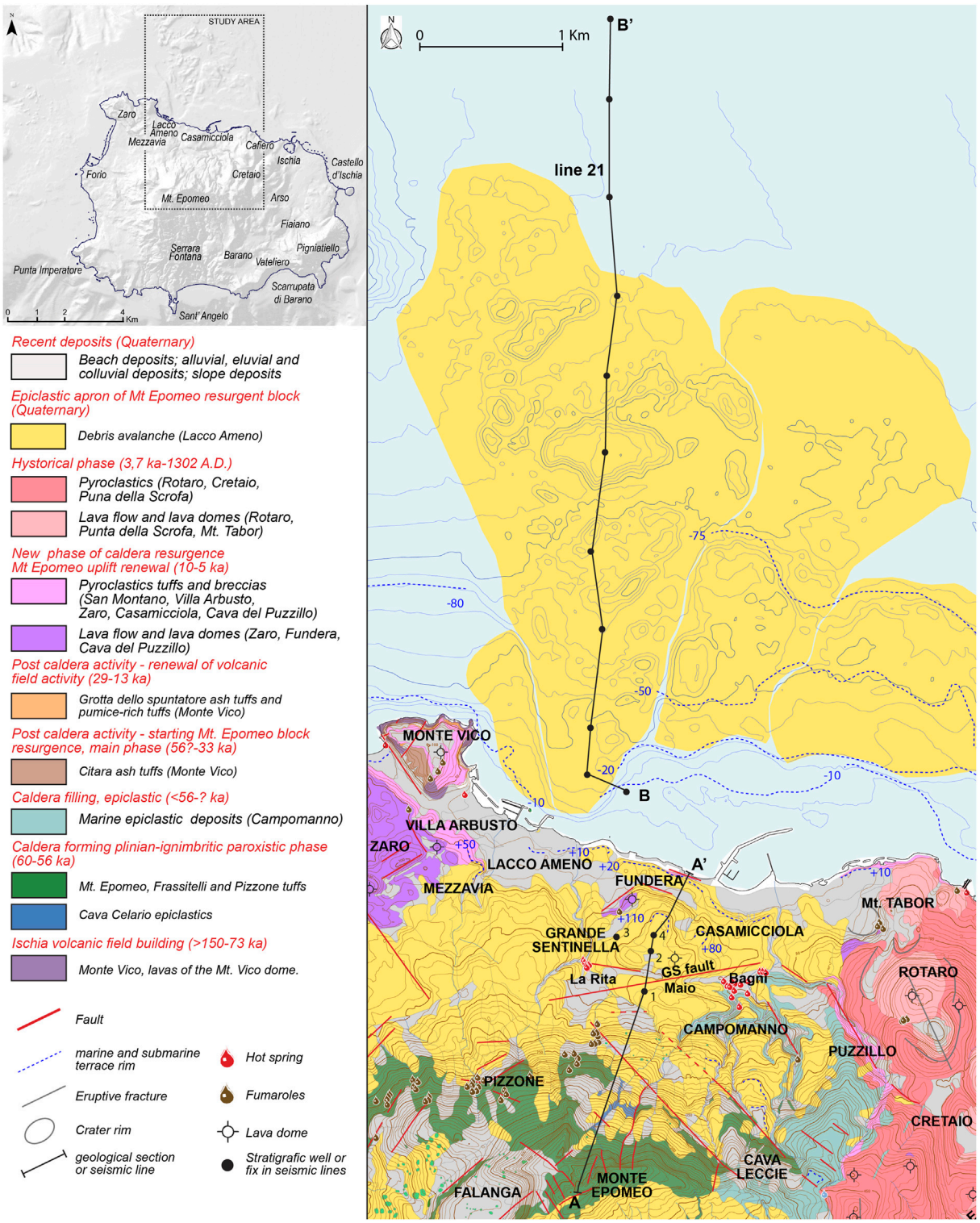


**FIGURE 2 |** Geological sketch of the northern sector of Ischia Island (Sbrana et al., 2018, modified).

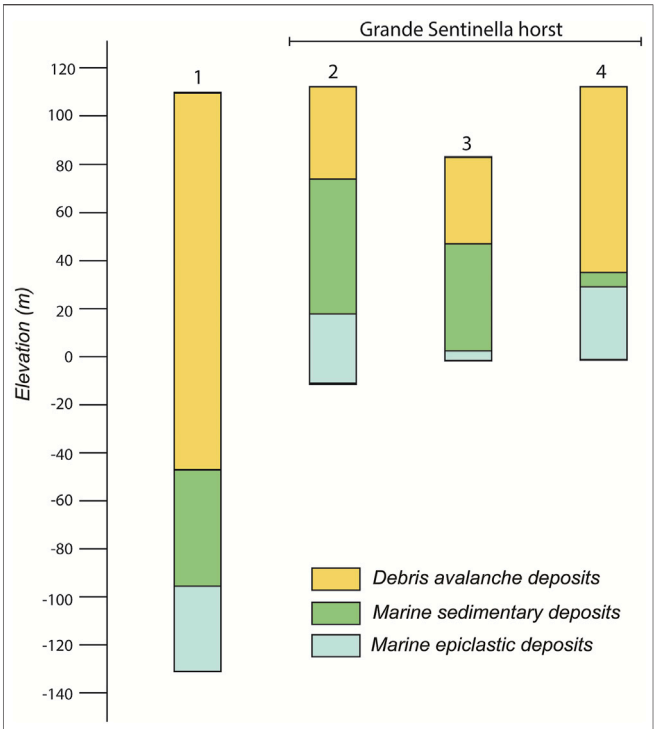


**FIGURE 3 |** Stratigraphy inferred from geothermal wells (1–4) located between Maio, La Rita, and Grande Sentinella sector (A–A' section, **Figure 2**). The interpretation of stratigraphy highlights the uplift of the oldest marine deposits (caldera filling sediments) in the Grande Sentinella sector. The location of the wells is indicated in **Figures 2**, **4** (see text for details).

lithological characters of volcanic and sedimentary and epiclastic geological bodies, applying the principle of continuity of on-land units, coastal units, and offshore marine units.

## Melt Inclusions

In general, melt inclusion (MI) investigations can provide significant information on the pre-eruptive settings (composition, temperature, and depth) of feeding system of volcanoes (Blundy and Cashman, 2005; Marianelli et al., 2006). Here MI analyses allowed us to obtain constrains about the depth and temperatures of magma feeding the northern sector of the island, during the final stage of volcanism (10 ka–1302 A.D.). Sample collection of juvenile fraction was restricted to trachytic pumices from fallout deposits of Cretaio Plinian eruption, to latitic scoriae from Vateliero scoria cone, and to latitic–trachytic banded pomiceous scoriae from Arso explosive/effusive eruption. The juvenile fractions show variable phenocryst content in a glassy matrix. Phenocrysts were handpicked, mounted on slides, and double polished. After petrographic inspection, selected MIs were prepared for further analyses. All the selected samples host melt inclusions having a glassy appearance. SEM-EDS microanalysis was carried out on MI and also on minerals and glasses using a Philips XL30 EDAX Genesis. Operating conditions were 20 kV and about 0.1 nA beam current. A raster area of about 100 $\mu m^2$ was employed for glass analysis to reduce the light element loss. The analyses were normalized to 100 wt% by using the EDAX software. A set of reference standard of natural trachytic (CFA47), basaltic (ALV981R23), and pantelleritic (KE12) glasses were analyzed before every session. Analytical results, errors, reproducibility, and detection limits using international standards for SEM-EDS technique are reported in Marianelli and Sbrana (1998).

Microthermometric homogenization experiments on MIs were carried out on doubly polished wafers of crystals. Only glassy MIs, with a clear shrinkage bubble and no evidence of heterogeneous trapping (Roedder, 1984), were chosen. For the high-temperature experimental study of MIs, a modified Leitz 1,350 heating stage was used. The temperature was measured with a Pt-Pt90Rh10 thermocouple. The accuracy of measurement was around ±10°C, controlled by the melting point of gold and silver. Experiments were performed in a He atmosphere. The rate of heating was varied as a function of the rate of transformation in the inclusions and ranged from 2°C to 40°C/min to the point of complete homogenization of MI, i.e., disappearance of bubbles. Pilot runs were carried out in order to define the correct heating/step procedure before the starting of thermometric data collection. Vapor loss can be excluded due to the reproducibility of experiments on the same MI.

$H_2O$ and $CO_2$ in MI were analyzed by transmission IR spectroscopy (FTIR) using a Nicolet iN10 equipped with a high-intensity EverGlo IR source and MCT-A detector cooled with liquid nitrogen. At least three spectra for different areas were collected for each MI (minimum area of 10 × 10 μm). The concentrations, C, were calculated according to the Beer–Lambert law: $C = 100 \cdot A \cdot M/(\varepsilon \cdot \rho \cdot d)$, where A (absorbance) is the peak height of the absorption in dimensionless absorbance units, M is the molar mass (g/mol), ε is the molar absorptivity ($l \cdot mol^{-1} \cdot cm^{-1}$), ρ is the density ($g/cm^3$) of glass (estimated using the iterative method of the Church and Johnson, 1980, and Gladstone–Dale rules), and d is the thickness measured by visual determination under a calibrated microscope, with an error of 2–3 μm depending on the proximity of a given inclusion to the edge of the wafer. The quantitative procedure and the absorption band assignments described in Silver et al. (1990) and Wallace et al. (1999) were followed in this work. The molar absorptivity values chosen were 62 for the 3,570 $cm^{-1}$ according to Di Matteo et al. (2004). No carbon peak is observable above the background, indicating that the $CO_2$ is below detection limit (about 50 ppm, depending on MI thickness).

# RESULTS

## Offshore and Onshore Geological Results

The map in **Figure 2** highlights the geological, geomorphological, and structural patterns of the Casamicciola area and its northern offshore sector. On land, north of Ischia, we observe an interdigitation of 1) thick volcanic units linked to the caldera-forming phase of the volcanic field, 2) clay-rich marine sedimentary bodies from Campanian plain, and 3) thick epiclastic units formed during the caldera filling and the successive resurgence.

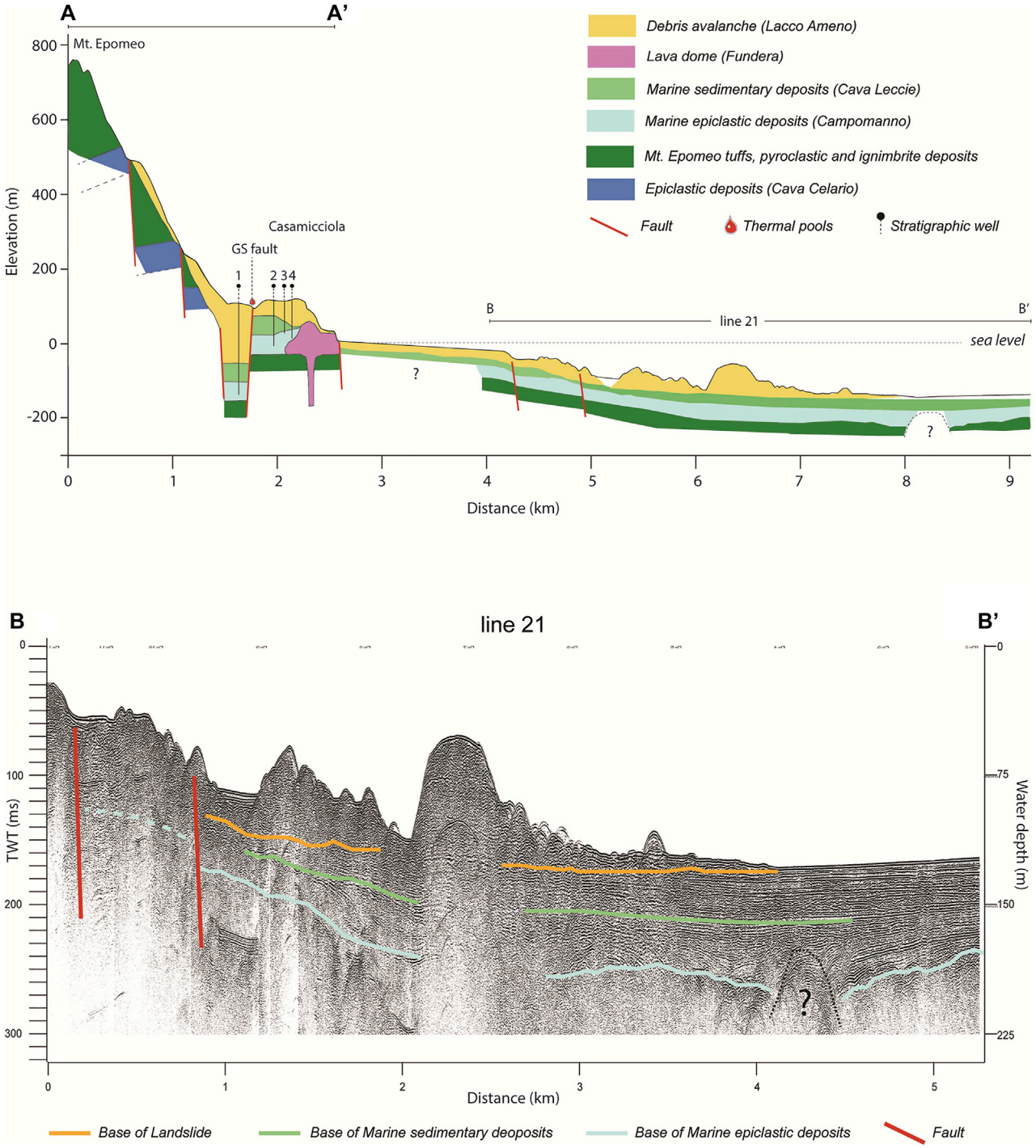


**FIGURE 4 | (A)** Volcanological sketch of the north side of Ischia Island (onland A–A' and offshore B–B' sections). one to four indicate the location of the wells illustrated in **Figure 3**. The offshore setting is based on the interpretation of the seismic line 21 (B-B') **(B)**.

The structural framework of the studied area is characterized by faults with vertical offsets that reach tens of meters, well evident in the geological section displayed in **Figure 4**, which includes the stratigraphy of the on-land wells (A–A′) and the interpretation of the seismic line (B–B′) offshore. The north portion of the seismic line (B–B′) appears undeformed, while several faults bordering marine terraces evidence a progressive uplift of the volcanic and sedimentary units toward the inland. The acoustic basement is represented by a unit having a characteristic reflection-free facies typical of ignimbrites (Aiello

et al., 2020). This is relatable to the caldera-forming phase (60–56 ka, Sbrana et al., 2018), in which thick ignimbrites are emplaced, including the Mt. Epomeo Green Tuff unit. The acoustic basement unit is topped by reflection rich seismic units, interpreted as corresponding to the sequence of epiclastics and clay-rich marine sediments covering the Ischia ignimbrite deposits, outcropping on the northeast slopes of Mt. Epomeo resurgent block (Campomanno epiclastics and Cava Leccie clays and sands, marine units).

These units and the underlying tuffs are arranged in several step faults accommodating the Epomeo uplift. On the other hand, in the marine area, they appear affected by a bending linked to a normal fault system that connects to the Grande Sentinella horst (**Figures 2** and **4**). In the on-land part, on this structure, the marine sediments are uplifted up to about 80 m a.s.l. Wells stratigraphy (Drilling 1 to 4, **Figure 3**) and morphostructural counterslope show the existence of a small graben placed between the Grande Sentinella horst and the Mt. Epomeo normal master fault (**Figure 3**) bordering the resurgent block.

Two deformation systems having different amounts of deformation are shown in the geological map (**Figure 2**) and in the land–sea section (**Figure 4**). The most deformed area, experiencing almost 900 m of uplift, coincides with the Mt. Epomeo block resurgence (56–33 ka post caldera activity); this is delimited by the north dipping normal fault of the Piazza Bagni–La Rita graben (**Figures 2** and **4**). Northward deformations are less developed (tens of meters) and the maximum uplift (about 100 m) coincides with the Grande Sentinella horst (**Figure 4**). This structure is part of the uplifted domed belt formed after 5 ka (during phases 5 and 6 of Sbrana et al., 2018), between Cafieri area, Casamicciola, and Mezzavia in the northern coastal sector of the volcanic field and highlighted by marine fossiliferous epiclastics units uplifted up to 50–80 m above sea level.

The presence of marine terraces, both on land and offshore (**Figure 4**), records several stages of deformation linked to fault activity and sea level variations in the northern sector of the island: in particular, four order of marine terraces are mapped offshore at −10, −20, −50, and −75/80 m b.s.l. (partially covered by the morphology of Lacco Ameno debris avalanche), while on land, terrace rims are located at 10, 20, 50, 80, and 110 m a.s.l., uplifted by the recent uplift in the Grande Sentinella, Casamicciola, Mezzavia, and Fundera areas.

## Petrological and Geochemical Results

Volcanism of the last 10 ka of activity (phases 5 and 6) is mainly concentrated on northern sectors of the island and is represented by lava domes, lava flows, and tuff cones. The volcanic products of Ischia are characterized by a strong alkalinity ($Na_2O + K_2O$ up to 14 wt.%) and the bulk rock composition ranges from latite to trachyte (**Supplementary Figure S1A**), with rare shoshonite and phonolite, as already reported by Rittman and Gottini (1980), Crisci et al. (1989), Civetta et al. (1991), Sbrana et al. (2018). Most of the erupted magmas are highly differentiated and consists of lava flows, lava domes, and pyroclastics trachytic in composition, with crystalline felsic xenoliths present in the pyroclastic units. However, petrochemical data (Piochi et al., 1999; Pelullo et al., 2020) highlight that mingling/mixing processes affect volcanic products of phase 5 (e.g., Zaro) and phase 6 (e.g., Fiaiano, 530–960 A.D., Arso, 1302 A.D. among the others) (**Figure 1**). Several studies agree with a relatively shallow magmatic system present in the island subsoil (Rittmann, 1930; Poli et al., 1987; Crisci et al., 1989; Civetta et al., 1991; Sbrana et al., 2009). The evidence of a shallow magmatic system is supported by the very high geothermal gradient measured in the island, by gravimetric, potential field, and magnetotelluric data (Nunziata and Rapolla. 1987; Paoletti et al., 2009; Sbrana et al., 2009; Di Giuseppe et al., 2017; Carlino, 2018); however, this system is still weakly defined.

In order to obtain reliable data from MI investigation, the juvenile fractions of Ischia volcanic deposits were selected, on the basis of cooling rate (Cioni et al., 1998). The selection was restricted to samples of pumice deposits. In particular, for the phase 6 volcanic activity, well-quenched primary two-phase glassy MIs (20–60 μm in size) are found in clinopyroxene of pumices and scoriae of the juvenile fraction of the Cretaio, Arso, and Vateliero eruptions. The mineralogical assemblage of their hosting rock is formed by K-feldspar, plagioclase, clinopyroxene, biotite, oxides, apatite, and titanite. The analyzed MIs have trachytic composition (**Supplementary Table S1** and **Supplementary Figure S1**); as the major element composition of most MIs is similar to that of the glassy matrix, this could indicate that only minor differentiation of melts occurred between entrapment and eruption. Microthermometric experiments provided a homogenization temperature between 956°C and 1,043°C, with a mode of 1,005°C (**Supplementary Figure S2**).

FT-IR investigation revealed that the dissolved water content ranges from 1.0 to 2.9 wt.% with a median value of 2.2 wt.%, (**Supplementary Table S2** and **Supplementary Figure S3**) similar to the range of values reported in Sbrana et al. (2009) for older eruptions (phase 4 and phase 2) of the southern sector of the Ischia volcanic field.

The dissolved water content of MIs can be assumed as representative of the pre-eruptive volatile content of melts. According to the hypothesis of water saturation conditions for the trapped melts, the $H_2O$ solubility model of Di Matteo et al. (2004) for trachytic melts was applied to calculate saturation pressure for these MIs and a pressure range of 17–52 MPa was obtained (**Supplementary Table S2** and **Supplementary Figure S4**). This pressure range, throughout a model based on measured densities of the rocks (from 1.5 to 2.0 $gcm^{-3}$ for hydrothermally altered tufaceous rocks, 2.4 to 2.5 $gcm^{-3}$ for fresh trachytes and syenites, Sbrana et al., 2009), is then converted to depth. Accordingly, MIs were trapped within a trachytic storage region located between 800 and 3,500 m from actual ground surface (<2.000 m, for the median value of saturation pressure; **Supplementary Figure S4** and **Supplementary Table S2**), at least in its shallower apophyses. Based on compositional (major elements and $H_2O$ content) and temperature data recorded by MIs, very low viscosity values (about $10^3$ Pa s, analogous to values known for basaltic melts) have been estimated for trachitic melts following the procedure of Giordano et al. (2008). Therefore, trachitic melt having relative high mobility can be hypothesized in the shallower portions of the Ischia magmatic feeding system, although the high crystal content

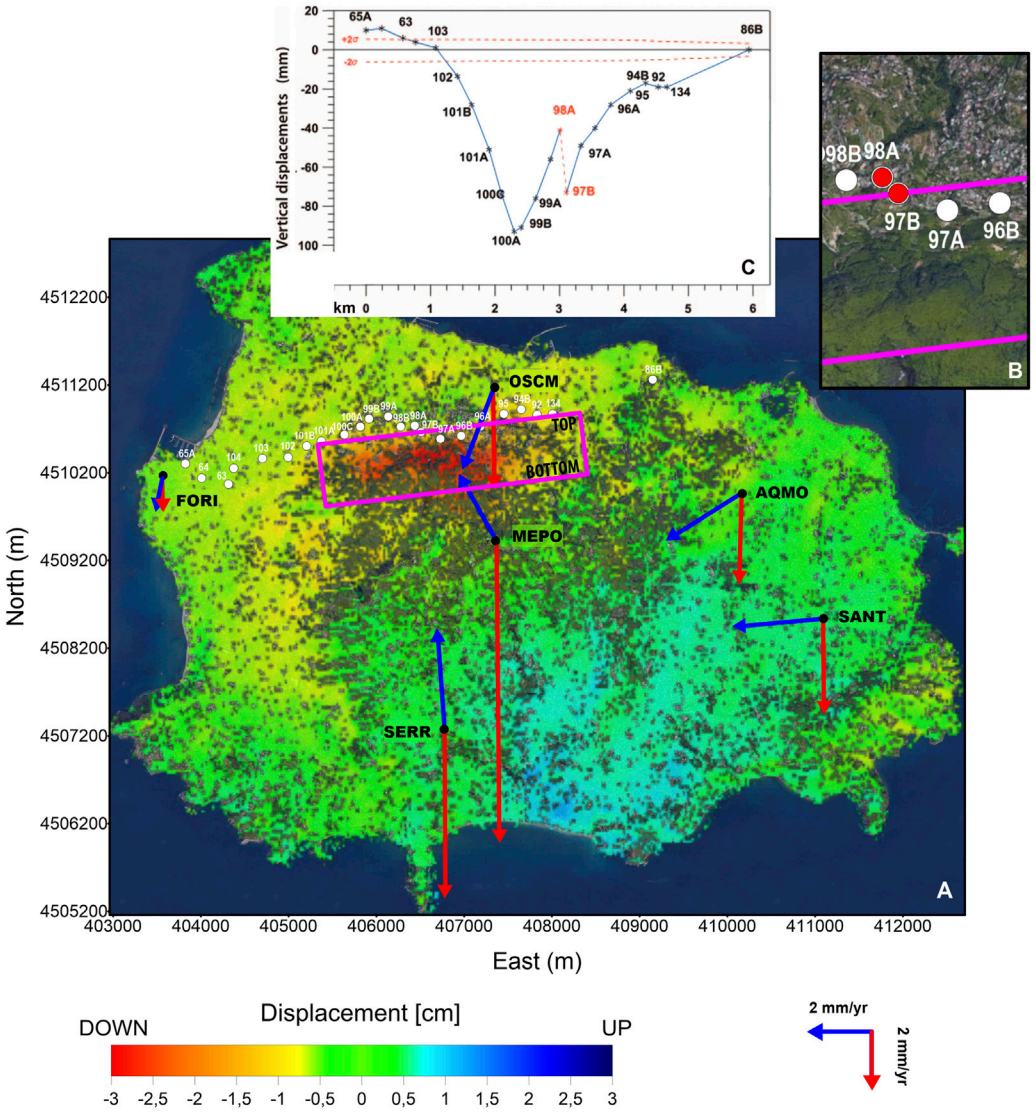


**FIGURE 5 |** Map of Ischia Island with indication of: **(A)** DInSAR vertical cosesimic displacement as shown in De Novellis et al. (2018); horizontal (blue arrows) and vertical (red arrows) GPS velocity field for Ischia Island in the time spam 2001–2019 (after De Martino et al., 2021); benchmarks of the high precision leveling network of INGV (white points); fault projection of 2017 earthquake as inferred by De Novellis et al. (2018) (purple rectangle and fault TOP and BOTTOM). **(B)** Particular of the fault projection across the benchmarks 97B and 98A. **(C)** coseismic displacement measured by the leveling survey after the 2017 earthquake (from Ricco et al., 2019).

of some volcanic products (e.g., Zaro) determines a significant change in magma rheology, such as increase in viscosity (Costa, 2005). The occurrence of felsic crystalline xenoliths in pyroclastic deposits testifies that also crystalline portions of magma chamber (solidification front of Marsh, 2000) and/or related intrusive or subvolcanic bodies are present in the shallower portion of the feeding system, together with low-viscosity melts. Furthermore, rare MIs in Arso and Vateliero samples have less differentiated composition and higher homogenization temperature, well in agreement with shoshonitic to basaltic melts rising from deeper storage zone (5–8 km of depth) and mixed with resident low-pressure trachytes (Piochi et al., 1999; Pelullo et al., 2020).

# DISCUSSION

## Relationship of Tectonic Structures With the Resurgence of Mt. Epomeo Block

The interpretation of seismic and the borehole data, joined with the CARG geological data show that the process of resurgence was characterized by different phases, which involved in a different fashion the outer and the inner part (Sbrana et al., 2011, 2018) of the present resurgent block. In the northern offshore, the presence of normal faults dipping northward, with small vertical throw (tens of meters) gradually increasing southward and cutting the deposits of eruptions following the caldera formation, indicates a differential uplift of the island

**TABLE 3 |** cGPS horizontal and vertical velocities for Ischia Island in the time spam 2001–2019 (De Martino et al., 2011).

| Station | Lat N | Long E | First observation (decimal year) | North vel (mm/year) | East vel (mm/year) | Up vel (mm/year) | North err (mm/year) | East err (mm/year) | Up err (mm/year) |
|---|---|---|---|---|---|---|---|---|---|
| AQMO | 40.736 | 13.935 | 2001.1 | −1.6 | −2.4 | −3.1 | 0.1 | 0.1 | 0.2 |
| FORI | 40.737 | 13.856 | 2005.4 | −1.1 | −0.2 | −1.3 | 0.1 | 0.1 | 0.2 |
| IPRO | 40.765 | 14.024 | 2004.2 | −1.7 | −3.3 | 0.0 | 0.1 | 0.1 | 0.2 |
| MEPO | 40.731 | 13.902 | 2017.1 | 2.3 | −1.3 | −11.2 | 0.2 | 0.2 | 1.0 |
| OSCM | 40.747 | 13.901 | 2011.0 | −2.9 | −1.1 | −3.6 | 0.1 | 0.1 | 0.2 |
| SANT | 40.723 | 13.946 | 2013.4 | −0.2 | −2.8 | −3.2 | 0.1 | 0.1 | 0.2 |
| SERR | 40.712 | 13.895 | 2001.1 | 3.6 | −0.2 | −6.1 | 0.1 | 0.1 | 0.2 |

(**Figure 4**). Assuming an about radial symmetry for the magmatic intrusion of Ischia (Carlino, 2012, and references therein), the location of the offshore faults related to the resurgence indicates a magmatic sill intrusion of about 5 km in diameter.

The faults characterized by larger vertical throw delimit the main uplifted structure of Mt. Epomeo, whose dislocated blocks appear slightly tilted southward, with evidence of uplift starting from Casamicciola–Grande Sentinella up to about 3.5 km north of the coastline (**Figure 4**). This structural pattern has been recognized in other resurgent calderas (i.e., Long Valley caldera: Bailey, 1989; Hildreth et al., 2017. Phlegrean caldera: Sbrana et al., 2021; Steinmann et al., 2018; Sacchi et al., 2014) as well as in experimental analog modeling of shallow magma intrusion (Walter and Troll, 2001; Acocella et al., 2004). A localized uplift appears to have occurred in the final stage of the resurgence, post 5 ka, involving the Casamicciola-Grande Sentinella sector, uplifted by about 100 m with respect to the sea level. This provides a relatively high average uplift rate of at least 1–2 $cm{\cdot}year^{-1}$.

The interpretation of borehole data highlights the dislocation of the oldest marine deposits (caldera filling sediments) encountered in the Hotel Tusculum (Drilling 1) and Pantano (Drilling 2) wells (**Figures 3**, **4**), being characterized by an offset of about 80 m between the top of the deposits (Cava Leccie fossiliferous clay and sands) in the two wells. These sediments are covered by quaternary Lacco Ameno debris avalanche deposits and debris flows (**Figure 4**).

According to the above observations, the southern sector of the Grande Sentinella uplifted block would have been cut by a roughly E-W normal fault (or faults system), for which there are also morpho-structural evidences (Sbrana et al., 2018). The formation of a graben-like structure—favored by the doming occurred in phases 5 and 6 and likely by the regional extensional tectonics (Hippolyte et al., 1994)—accommodates the dislocation occurring along a southward dipping fault (**Figure 4**). This structure appears not to be related (spatially nor chronologically) to the main resurgence phase of the Mt. Epomeo. This hypothesis is supported by the roughly E-W alignments of most recent eruptive centers at Casamicciola (Grande Sentinella-Mezzavia-Fundera) and by the MI data indicating a very shallow depth (mean value <2,000 m) of the magma bodies along the northern sector and outside the resurgent block. We suggest that the graben-like structure was originated when magma migrated at a shallower depth (as indicated by MI data) in the northern sector about 10–5 ka, in the final stage of the resurgence. The different patterns of ground deformation and the related structural pattern might be associated with the different evolution of the intrusion dynamics. At Ischia, the change in pattern of deformation possibly reflects a complex shape of the underlying magma intrusions. For instance, steeper edges of the uplifted zones are generally located above the shallower parts of the intrusion (Galland, 2012), as confirmed at Ischia by geophysical investigations (Di Giuseppe et al., 2017). During the most recent geological history of the island (10–5 ka), the pattern of magma migration in the northern sectors might have been controlled by the presence of roughly vertically dipping faults related to the resurgence, along which dike migration up to the surface is favored by extensional tectonics (Piochi et al., 2005; Torrente et al., 2010; Gudmundsson, 2020). On the other side, the onset of the subsidence process may have squeezed out a fraction of the resident magma in the shallow source (Gudmundsson, 2020). This process, possibly starting after 5 ka, enhanced magma displacement toward the surface, generating localized uplifts. Furthermore, the petrological data show a contemporary presence of low and high crystalline magma batches in the shallow source of Ischia. These data suggest that the higher viscosity of the resident magma may have not favored the magma hybridization with the mostly basaltic, less viscous, magma that raised from the depth of about 5–8 km without residing in the shallow source (e.g., Arso and Vateliero eruptions); indeed, the interaction between magmas with different viscosity results only in the observed sporadic mingled products.

The horst-graben structure and the related fault dislocating the northern block of the Grande Sentinella represent crucial volcano-tectonic features, since they correspond to the seismic zone of the island generating the destructive earthquakes in historical and recent time (Carlino et al., 2021). The lateral and vertical extension of this seismogenic zone is controlled by the dimension of the resurgent block of Mt. Epomeo and the depth of brittle–ductile transition, respectively (Carlino et al., 2021). Thus, the fault appears enclosed into a complex kinematics, where the resurgence in a former phase and the subsequent subsidence have generated an intricated volcano-tectonic system, on a relatively small area. Reconstructing the past deformations and measuring the present ground movements are thus crucial to understand the island dynamics and the associated seismicity.

## Relationship of Tectonic Structures With Seismicity and Recent Deformation

The 2017 earthquake was the first considerable event in the island recorded instrumentally according to modern standards. It

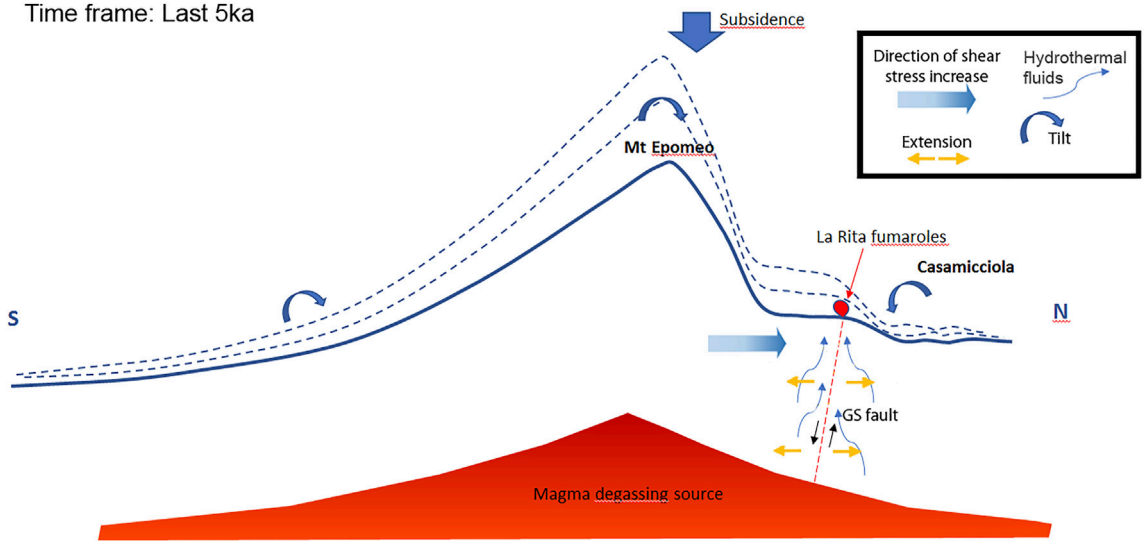


**FIGURE 6 |** Qualitative sketch of the geological processes favoring the activation of the Grande Sentinella (GS) fault (N-S profile, NOT TO SCALE). Round thick arrows (in blue) indicate the slight tilting of the block inferred from horizontal component of the GPS stations. Dotted lines (in blue) indicate the former profile position (see text for details).

provided the possibility to obtain a quantitative model of the seismic fault from the analysis of geodetic and seismic data (De Novellis et al., 2018). The solution is characterized by an almost purely normal fault plane, with most dislocation concentrated on an area of about 1.5 × 1 $km^2$, slightly dipping southward (70° ± 7°), with strike 86° ± 5° and rake −80° ± 5°, located at the northern base of Mt. Epomeo and with its top at about 400 m below free surface (De Novellis et al., 2018). The higher accuracy of the location of the fault retrieved by De Novellis et al. (2018) with respect to other proposed solutions (see for instance Braun et al., 2018, and Calderoni et al., 2019) is demonstrated by the result of the high-precision leveling survey performed by INGV immediately after the 2017 earthquake (Ricco et al., 2019). In fact, the surface projection of the fault runs through the 97B and 98A leveling benchmarks, where a 3.2-cm offset associated to the coseismic displacement of the 2017 fault was detected by the survey (**Figure 5**). According to Carlino et al. (2021), this is the fault responsible for the historical and recent earthquakes of the island. Based on its location, geometry, and kinematics, this seismogenic structure is consistent with the southward dipping Grande Sentinella (GS) fault, bordering the graben structure described above.

In this framework, the GS fault would act in response to the local stress field associated with the subsidence of the Mt. Epomeo block, which represents the stress load mechanism (De Novellis et al., 2018; Trasatti et al., 2019; Carlino et al., 2021) and appears to be active since historical time. In fact, the ground deformation records show that at least the northern coastline experienced subsidence since about 2 ka, with rate of the order of a few millimeters per year (Buchner et al., 1996). Besides, the present measurements–as recorded since at least 30 years from the INGV GPS and leveling surveillance networks and from DInSAR data (Manzo et al., 2006; De Martino et al., 2011; De Novellis et al., 2018)—indicate a general subsidence of the island with a similar rate, between 1 and 11 mm $yr^{-1}$.

Focusing on the most recent ground deformation patterns, the horizontal velocity field derived from the continuous GPS stations operating on the island (**Figure 5**) evidences that in the eastern part the horizontal displacements are mainly westward, with rates of about 3 mm $year^{-1}$ (De Martino et al., 2021). The FORI station, located in western part of the island, outside the caldera structure, shows negligible horizontal trend, indicating a condition of greater stability in this part of the island (De Martino et al., 2021). The horizontal velocity vector at MEPO (2.6 mm $year^{-1}$), located at the top of Mt. Epomeo, shows velocity pointing toward NNW, while OSCM, in the north part of the island, has a rate of about 3 mm $year^{-1}$ in direction SW (De Martino et al., 2021). On the other hand, vertical deformations recorded by GPS, DInSAR, and leveling data highlight an increasing subsidence rate going toward the center of the island, with the maximum rate recorded at MEPO (11 mm $year^{-1}$) (**Figure 5** and **Table 3**).

## A Conceptual Volcano-Tectonic Model of the Island

The GS fault represents the boundary between the main resurgent zone, to the south, presently subsiding, and a relatively less subsiding area along the coast of Casamicciola, to the north. This subsidence trend could have activated extensional structures at the border of the resurgent dome (Walter and Troll., 2001). Furthermore, the overall GPS measurements indicate the sinking of Mt. Epomeo with a slight northward tilt of the block, consistently with Trasatti et al. (2019). This pattern suggests that the maximum shear stress related to the concurrent effect of tilting and differential subsidence must be located at the northern base of the central block, somewhere in between MEPO and OSCM. The GS fault is located between these stations.

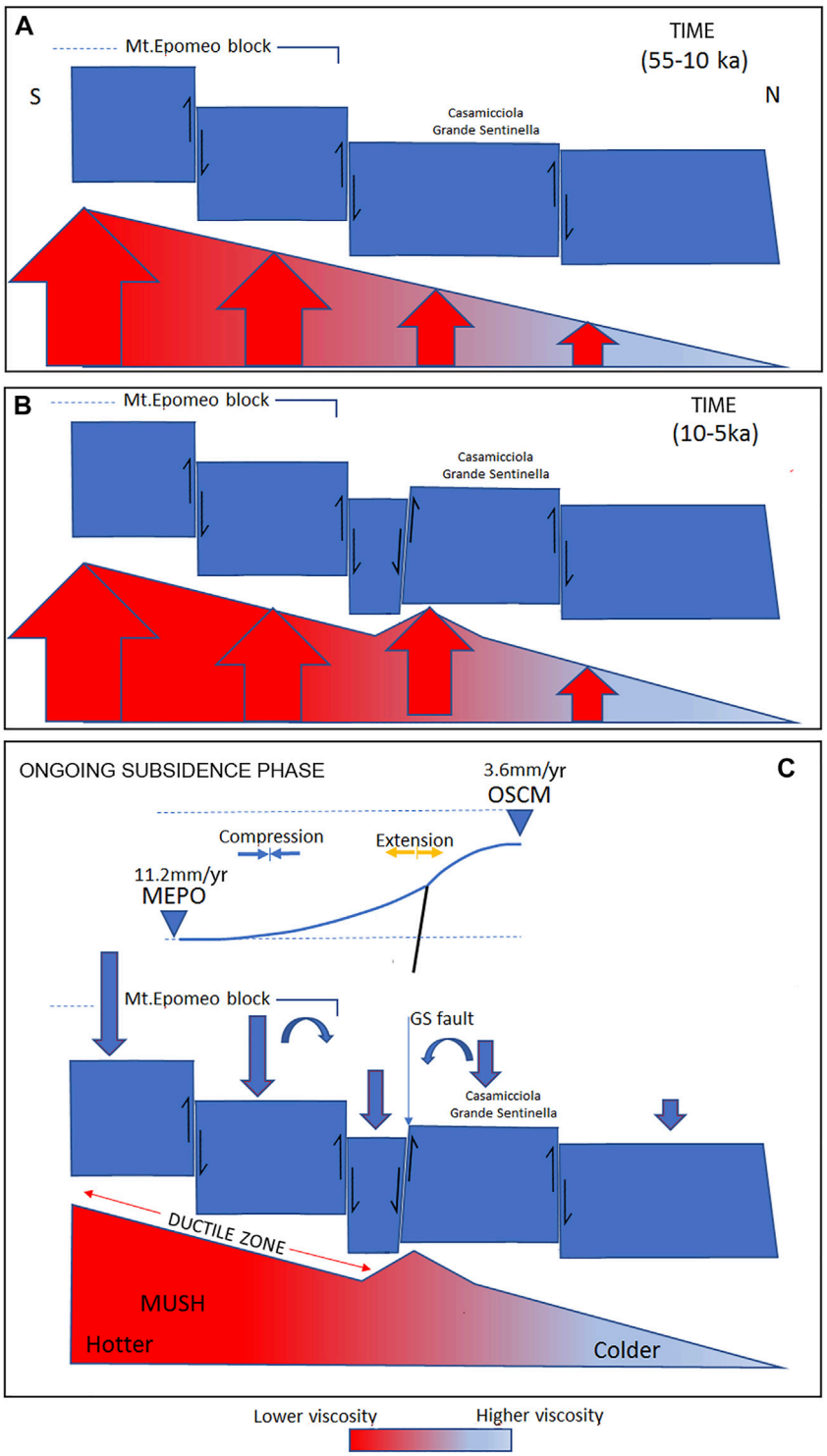


**FIGURE 7 |** Conceptual sketch of faults formation during the earlier (55–10 ka) and late (10–5 ka) stage of the resurgence [panels **(A,B)**, respectively] and the present dynamic that is characterized by subsidence panel **(C)**. Red arrows in the panel A and B indicate the magma pressure exerted on the rigid block: increasing dimension indicates larger pressure. In the late stage of the resurgence, further magma arrived in the system and dislocated the block of Grande Sentinella upward along a fault which lowered a small southern block forming a local host-graben-like structure panel **(B)**. Panel **(C)** shows a qualitative deformation profile as function of the differential downward movement (blue arrows) between the MEPO and OSCM GPS stations. Curved arrows indicate the slight sinking of the blocks inferred from horizontal component of the GPS benchmarks. NOT TO SCALE (see text for details).

These observations suggest that during the present subsidence phase the activation of the faults located at the northern base of the Mt. Epomeo block can be favored by the increase of shear stress (**Figure 6**). Moreover, the main hot springs—located in the Casamicciola area (Bagni-La Rita-Maio) (**Figure 6**)—are aligned along the GS fault, which likely operates as a fluids discharge zone of the shallow geothermal system (Chiodini et al., 2004; Carlino et al., 2014; Trasatti et al., 2019). This could facilitate fault slipping due to the significant reduction of the effective stress (Sibson, 1981), favoring dislocation on this structure rather than on the southern side of the graben.

In the light of the new data and according to previous models of resurgence at Ischia (Carlino et al., 2006; Sbrana et al., 2009; Carlino, 2012), we suggest the following conceptual scheme of island resurgence (**Figure 7**): the onset of a magmatic intrusion (occurred after caldera formation) at a few (2–3) kilometers of depth (Sbrana et al., 2009; Paoletti et al., 2013; Di Giuseppe et al., 2017) produced the initial uplift of a large portion of the island, about 10 km in diameter, and the onset of faulting related to the resurgence. As magma injected proceeded and the volume has grown, the intrusion did not extend anymore, due to crystallization of the periphery (Pagie, 1913), and active pushing was exerted by the central part of the intrusion (the present Mt. Epomeo block), as a piston stage (Carlino, 2012). This process generated a pervasive fracturing, while the displacement of the central block occurred along the faulting at its boundary, where volcanic activity took place. Moreover, at Ischia Island, it is observed that the available magmatic energy was largely dissipated through uplift, rather than eruptions (Acocella and Funiciello, 1999). Assuming a minimum magma volume of at least 10 $km^3$ to generate the uplift of the Mt. Epomeo block (Carlino, 2012; Galetto et al., 2017) and giving the erupted volume emitted after the caldera collapse, which is less than 0.1 $km^3$ (Carlino, 2012 and references therein), a very high intrusive/eruptive ratio is found. This observation supports the hypotheses of low mobility of the resident magma and possibly its high viscosity acted as a barrier for new magma to erupt (Galetto et al., 2017). In this case, as suggested by Galetto et al. (2017), magma could be injected at the boundary of the more viscous zone. We suggest that this process occurred in the final stage of resurgence, when the arrival of new magma (Civetta et al., 1991) has migrated along the eastern and northern boundary of the resurgent structure (Sbrana et al., 2018). We also suggest that the onset of subsidence (<5 ka) may have further squeezed out a fraction of the resident magma facilitating its movement toward the surface (Gudmundsson, 2020) and possibly triggering a part of the most recent volcanic activity (phase 6) in the Island. In the northern sector, between the base of the resurgent block and the Grande Sentinella, magma bulging dislocated two blocks, which formed the presently active seismogenic structure of the island. The northern block was uplifted (about 100 m) at a rate of 2 cm $year^{-1}$ at least, while the southern one subsided by about 50 m at about half rate (~1 cm $year^{-1}$). At the end of the resurgence and with the inversion of ground movement of the Mt. Epomeo block, the slow subsidence (a few mm $year^{-1}$) progressively accumulated vertical shear stress along the border of a sinking zone, between the two GPS stations MEPO and ECSM, which show a differential vertical deformation of about 7.6 mm $y^{-1}$. The 2017 earthquake was not preceded, neither followed, by any geophysical signals (e.g., deformation, gravity variations, and foreshocks) indicating possible movement of magma at shallow depth (De Novellis et al., 2018; Berrino et al., 2021). Furthermore, the similarity of this event with historical ones at Ischia in terms of distribution of felt reports, and source location, extension, and kinematics (Carlino et al., 2021) points to the same process as origin of the earthquakes, suggesting that no magma movement is involved in the generation of these earthquakes. We conclude that the faster long-term subsidence of the Mt. Epomeo block, resulting in differential vertical deformation, originates recurrent seismic reactivation of the inward dipping GS normal fault. The differential subsidence rate has been explained in terms of different response of a viscous layer to the loading of the overburden (Castaldo et al., 2017) or to the deflation and contraction of a silt-like source below Mt. Epomeo (Galvani et al., 2021).

## CONCLUSION

After long-term resurgence of about 1,000 m lasting about 50 kyr, the island of Ischia experienced a generalized subsidence—at least in historical time–and low-magnitude but high-intensity earthquakes, which occurred in the northern sector, along volcano-tectonic structures formed during the most recent uplift phase (Sbrana et al., 2018). In this framework, we focused on the analysis of this area, the most active of the island at present, and examined the pattern and the dislocation of both off-shore and on-land faults, using seismic profiles and boreholes data. New MI and geochemical data are also used to integrate our analyses.

We recognize an initial phase of the resurgence involving marginally the north off-shore zone of the island, which appears only modestly uplifted and allowed us to infer a possible diameter of about 5 km for the sill producing the initial resurgence. Most important, we identify a local horst-graben structure, formed in the final stage of the resurgence (5–10 ka), that includes the main seismogenic fault of the island, the Grande Sentinella (GS) fault. This structure is the source of historical and recent earthquakes of Ischia (De Novellis et al., 2018; 2019; Carlino et al., 2021). Its present dynamics is correlated with the ongoing subsidence of Mt. Epomeo. In this framework, the GS fault operated as a decoupling plane between the faster subsiding zone, the Mt. Epomeo block, and the slower subsiding zone of Casamicciola (**Figures 5** and **6**). We suggest that the extensional mechanism of the GS fault is favored by the differential stretching of the crust between the Mt. Epomeo and Grande Sentinella. On the other side, the opposite direction of the GPS horizontal components of Grande Sentinella and Mt. Epomeo stations could also indicate a slow gravitational sliding of the two different blocks along the graben extensional structure.

Furthermore, the GS fault activation is likely facilitated by the intense fluids' circulation (Chiodini et al., 2004; Carlino et al., 2014; Di Giuseppe et al., 2017), which reduces the normal stress on the fault plane.

As also evidenced by Trasatti et al. (2019) the case of Ischia island shows that shallow volcano-tectonic structures originated during the resurgence can release seismic energy during quiescent and/or subsiding phases linked to the evolution of volcano shallow feeding system, with significant seismic hazard, even though not related to magma movement in the shallow crust (De Novellis et al., 2018) but simply to lithostatic re-equilibration. In spite of their relatively limited dimension, generating small to medium earthquakes, the shallowness of these structures may give rise to elevated intensities (Cubellis and Luongo, 1998; Selva et al., 2019; Carlino et al., 2021).

As suggested by De Novellis et al. (2018) and Trasatti et al. (2019), the subsidence operates as mechanism of stress recharge on the seismogenic structures bordering the northern side of Mt. Epomeo. Thus, the potential for damaging earthquakes will remain high as long as the subsidence will operate (Trasatti et al., 2019). According to our analyses, the accumulated stress is mainly released along the GS fault, where the 2017 event originated (De Novellis et al., 2018) and where the most destructive historical earthquakes likely occurred (Carlino et al., 2021; Selva et al., 2021). A better knowledge of the mode of stress loading and release during the seismic cycles would provide elements for a better definition of the seismic hazard.

The process driving the subsidence has been explained through the coupling of crust rheology and gravitational loading of the resurgent block (Castaldo et al., 2017) and/or as the effect of slow depressurization of the shallow hydrothermal or magmatic system (Sepe et al., 2007; Trasatti et al., 2019; Galvani et al., 2021). We highlight that, our conceptual model of stress accumulation on the GS fault is independent of the processes driving the subsidence, which are instead fundamental in determining the times of stress loading. Finally, given the very high geothermal gradient of this area, higher than 180°C $km^{-1}$ (Carlino, 2019), we suggest that the presence of shallow ductile layer at a depth of 2–2.5 km (Castaldo et al., 2017) could have a strong control on the deformation rate and pattern of the different blocks forming the Mt. Epomeo loading structure.

## DATA AVAILABILITY STATEMENT

The original contributions presented in the study are included in the article/**Supplementary Material**, further inquiries can be directed to the corresponding author.

## AUTHOR CONTRIBUTIONS

AS, GP, and PM contributed to the data acquisition and interpretation. PD and VD provided the GPS and DInSAR data, respectively, and discussed about the ongoing deformation of the island. NP provided a contribution about the fault cinematic and the conceptual model of the island. SC wrote the paper and interpreted the data for the definition of the conceptual model of the island, with contribution from all the authors.

## FUNDING

This work was financed by "Dipartimento Scienze della Terra Università di Pisa" (Alessandro Sbrana). Part of data used in this paper have been acquired in the framework of the CARG project (https://www.isprambiente.gov.it/it/progetti/cartella-progetti-in-corso/suolo-e-territorio-1/progetto-carg-cartografia-geologica-e-geotematica/index).

## ACKNOWLEDGMENTS

We are grateful to the three reviewers and the Chief Editor Valerio Acocella for their helpful comments that improved the quality of the paper.

## SUPPLEMENTARY MATERIAL

The Supplementary Material for this article can be found online at: https://www.frontiersin.org/articles/10.3389/feart.2022.730023/full#supplementary-material

## REFERENCES

Acocella, V., Di Lorenzo, R., Newhall, C., and Scandone, R. (2015). An Overview of Recent (1988 to 2014) Caldera Unrest: Knowledge and Perspectives. *Rev. Geophys.* 53 (3), 896–955. doi:10.1002/2015rg000492

Acocella, V., Funiciello, R., Marotta, E., Orsi, G., and De Vita, S. (2004). The Role of Extensional Structures on Experimental Calderas and Resurgence. *J. Volcanology Geothermal Res.* 129 (1-3), 199–217. doi:10.1016/s0377-0273(03)00240-3

Acocella, V., and Funiciello, R. (1999). The Interaction between Regional and Local Tectonics during Resurgent Doming: the Case of the Island of Ischia, Italy. *J. Volcanology Geothermal Res.* 88, 109–123. doi:10.1016/s0377-0273(98)00109-7

Aiello, G., Iorio, M., Molisso, F., and Sacchi, M. (2020). Integrated Morpho-Bathymetric, Seismic-Stratigraphic, and Sedimentological Data on the Dohrn Canyon (Naples Bay, Southern Tyrrhenian Sea): Relationships with Volcanism and Tectonics. *Geosciences* 10 (8), 319. doi:10.3390/geosciences10080319

Bailey, R. A. (1989). I-1933.Geologic Map of Long Valley Caldera, Mono Inyo Volcanic Chain, and Vicinity, Eastern California. U.S. Geological Survey. Available at: https://ngmdb.usgs.gov/Prodesc/proddesc_15.htm.

Berrino, G., Vajda, P., Zahorec, P., Camacho, A. G., De Novellis, V., Carlino, S., et al. (2021). Interpretation of Spatiotemporal Gravity Changes Accompanying the Earthquake of 21 August 2017 on Ischia (Italy). *Contrib. Geophys. Geod.* 51 (4), 345–371. doi:10.31577/congeo.2021.51.4.3

Blundy, J., and Cashman, K. (2005). Rapid Decompression-Driven Crystallization Recorded by Melt Inclusions from Mount St. Helens Volcano. *Geol* 33, 793–796. doi:10.1130/g21668.1

Branney, M., and Acocella, V. (2015). "Calderas," in *The Encyclopedia of Volcanoes* (Academic Press), 299–315. doi:10.1016/b978-0-12-385938-9.00016-x

Braun, T., Famiani, D., and Cesca, S. (2018). Seismological Constraints on the Source Mechanism of the Damaging Seismic Event of 21 August 2017 on Ischia Island (Southern Italy). *Seismol. Res. Lett.* 89, 1741–1749. doi:10.1785/0220170274

Brown, R. J., Orsi, G., and de Vita, S. (2008). New Insights into Late Pleistocene Explosive Volcanic Activity and Caldera Formation on Ischia (Southern Italy). *Bull. Volcanol* 70 (5), 583–603. doi:10.1007/s00445-007-0155-0

Buchner, G., Italiano, A., and Vita-Finzi, C. (1996). "Recent Uplift of Ischia, Southern Italy," in *Volcano Instability on the Earth and Other Planets*. Editors W. J. McGuire, A. P. Jones, and J. Neuberg (London: Geological Society London Special Publications), 110, 249–252. doi:10.1144/gsl.sp.1996.110.01.19

Calderoni, G., Di Giovambattista, R., Pezzo, G., Albano, M., Atzori, S., Tolomei, C., et al. (2019). Seismic and Geodetic Evidences of a Hydrothermal Source in the Md 4.0, 2017, Ischia Earthquake (Italy). *J. Geophys. Res. Solid Earth* 124, 5014–5029. doi:10.1029/2018jb016431

Carlino, S., Cubellis, E., Luongo, G., and Obrizzo, F. (2006). "On the Mechanics of Caldera Resurgence of Ischia Island (Southern Italy)," in *Mechanisms of Activity and Unrest at Large Calderas*. Editors C. Troise, G. De Natale, and C. R. J. Kilburn (London: Geological SocietySpecial), Vol. 269. doi:10.1144/gsl.sp.2006.269.01.12

Carlino, S., Cubellis, E., and Marturano, A. (2010). The Catastrophic 1883 Earthquake at the Island of Ischia (Southern Italy): Macroseismic Data and the Role of Geological Conditions. *Nat. Hazards* 52, 231–247. doi:10.1007/s11069-009-9367-2

Carlino, S. (2018). Heat Flow and Geothermal Gradients of the Campania Region (Southern Italy) and Their Relationship to Volcanism and Tectonics. *J. Volcanology Geothermal Res.* 365, 23–37. doi:10.1016/j.jvolgeores.2018.10.015

Carlino, S., Pino, N. A., Tramelli, A., De Novellis, V., and Convertito, V. (2021). A Common Source for the Destructive Earthquakes in the Volcanic Island of Ischia (Southern Italy): Insights from Historical and Recent Seismicity. *Nat. Hazards*, 1–25. doi:10.1007/s11069-021-04675-z

Carlino, S., Somma, R., Troiano, A., Di Giuseppe, M. G., Troise, C., and De Natale, G. (2014). The Geothermal System of Ischia Island (Southern Italy): Critical Review and Sustainability Analysis of Geothermal Resource for Electricity Generation. *Renew. Energ.* 62, 177–196. doi:10.1016/j.renene.2013.06.052

Carlino, S. (2012). The Process of Resurgence for Ischia Island (Southern Italy) since 55 Ka: the Laccolith Model and Implications for Eruption Forecasting. *Bull. Volcanol* 74 (5), 947–961. doi:10.1007/s00445-012-0578-0

Castaldo, R., Gola, G., Santilano, A., De Novellis, V., Pepe, S., Manzo, M., et al. (2017). The Role of Thermo-Rheological Properties of the Crust beneath Ischia Island (Southern Italy) in the Modulation of the Ground Deformation Pattern. *J. Volcanology Geothermal Res.* 344, 154–173. doi:10.1016/j.jvolgeores.2017.03.003

Chiodini, G., Avino, R., Brombach, T., Caliro, S., Cardellini, C., De Vita, S., and Ventura, G. (2004). Fumarolic and Diffuse Soil Degassing West of Mount Epomeo, Ischia, Italy. *J. Volcanology Geothermal Res.* 133 (1-4), 291–309. doi:10.1016/s0377-0273(03)00403-7

Church, B. N., and Johnson, W. M. (1980). Calculation of the Refractive index of Silicate Glasses from Chemical Composition. *Geol. Soc. America Bull.* 91 (10), 619–625. doi:10.1130/0016-7606(1980)9110.1130/0016-7606(1980)91<619:cotrio>2.0.co;2

Cioni, R., Marianelli, P., and Santacroce, R. (1998). Thermal and Compositional Evolution of the Shallow Magma chambers of Vesuvius: Evidence from Pyroxene Phenocrysts and Melt Inclusions. *J. Geophys. Res.* 103, 18277–18294. doi:10.1029/98jb01124

Civetta, L., Gallo, G., and Orsi, G. (1991). Sr- and Nd-Isotope and Trace-Element Constraints on the Chemical Evolution of the Magmatic System of Ischia (Italy) in the Last 55 Ka. *J. Volcanology Geothermal Res.* 46, 213–230. doi:10.1016/0377-0273(91)90084-d

Costa, A. (2005). Viscosity of High crystal Content Melts: Dependence on Solid Fraction. *Geophys. Res. Lett.* 32, a–n. doi:10.1029/2005GL024303

Crisci, G. M., De Francesco, A. M., Mazzuoli, R., Poli, G., Stanzione, D., Cole, J. W., et al. (1989). Geochemistry of the Recent Volcanics of Ischia Island, Italy: Evidences of Crystallization and Magma Mixing. Chemical GeologyCalderas and Caldera Structures: a Review. *Earth-Science Rev.* 69 (1-2), 1

Cubellis, E., and Luongo, G. (1998). "Il terremoto del 28 luglio 1883. Danni, vittime ed effetti al suolo," in *Il terremoto del 28 luglio 1883 a Casamicciola nell'Isola d'Ischia* (Roma: Istituto Poligrafico e Zecca dello Stato), 59–100.

De Alteriis, G., Insinga, D. D., Morabito, S., Morra, V., Chiocci, F. L., Terrasi, F., et al. (2010). Age of Submarine Debris Avalanches and Tephrostratigraphy Offshore Ischia Island, Tyrrhenian Sea, Italy. *Mar. Geology.* 278 (1-4), 1–18. doi:10.1016/j.margeo.2010.08.004

De Martino, P., Dolce, M., Brandi, G., Scarpato, G., and Tammaro, U. (2021). The Ground Deformation History of the Neapolitan Volcanic Area (Campi Flegrei Caldera, Somma-Vesuvius Volcano, and Ischia Island) from 20 Years of Continuous GPS Observations (2000-2019). *Remote Sensing* 13, 2725. doi:10.3390/rs13142725

De Martino, P., Tammaro, U., Obrizzo, F., Sepe, E., Brandi, G., D'Alessandro, A., et al. (2011). La rete GPS dell'isola d'Ischia: Deformazioni del suolo in un'area vulcanica attiva (1998–2010). *Quaderni di Geofisica*, 95

De Novellis, V., Carlino, S., Castaldo, R., Tramelli, A., De Luca, C., Pino, N. A., et al. (2018). The 21 August 2017 Ischia (Italy) Earthquake Source Model Inferred from Seismological, GPS, and DInSAR Measurements. *Geophys. Res. Lett.* 45, 2193–2202. doi:10.1002/2017gl076336

De Novellis, V., Carlino, S., Castaldo, R., Tramelli, A., De Luca, C., Pino, N. A., et al. (2019). Comment on "The 21 August 2017 Md 4.0 Casamicciola Earthquake: First Evidence of Coseismic Normal Surface Faulting at the Ischia Volcanic Island" by Nappiet al.2018. *Seism. Res. Lett.* 90, 313–315. doi:10.1078/0220180231

de Vita, S., Sansivero, F., Orsi, G., Marotta, E., and Piochi, M. (2010). Volcanological and Structural Evolution of the Ischia Resurgent Caldera (Italy) over the Past 10 Ka. *Geol. Soc. Am. Spec. Pap.* 464, 193–239.

Di Giuseppe, M. G., Troiano, A., and Carlino, S. (2017). Magnetotelluric Imaging of the Resurgent Caldera on the Island of Ischia (Southern Italy): Inferences for its Structure and Activity. *Bull. Volcanol* 79 (12), 85. doi:10.1007/s00445-017-1170-4

Di Matteo, V., Carroll, M. R., Behrens, H., Vetere, F., and Brooker, R. A. (2004). Water Solubility in Trachytic Melts. *Chem. Geology.* 213, 187–196. doi:10.1016/j.chemgeo.2004.08.042

Galetto, F., Acocella, V., and Caricchi, L. (2017). Caldera Resurgence Driven by Magma Viscosity Contrasts. *Nat. Commun.* 8 (1), 1–11. doi:10.1038/s41467-017-01632-y

Galland, O. (2012). Experimental Modelling of Ground Deformation Associated with Shallow Magma Intrusions. *Earth Planet. Sci. Lett.* 317-318, 145–156. doi:10.1016/j.epsl.2011.10.017

Galvani, A., Pezzo, G., Sepe, V., and Ventura, G. (2021). Shrinking of Ischia Island (Italy) from Long-Term Geodetic Data: Implications for the Deflation Mechanisms of Resurgent Calderas and Their Relationships with Seismicity. *Remote Sensing* 13 (22), 4648. doi:10.3390/rs13224648

Giordano, D., Russell, J. K., and Dingwell, D. B. (2008). Viscosity of Magmatic Liquids: a Model. *Earth Planet. Sci. Lett.* 271, 123–134. doi:10.1016/j.epsl.2008.03.038

Gudmundsson, A. (2020). *Volcanotectonics: Understanding the Structure, Deformation and Dynamics of Volcanoes*. Cambridge University Press

Hildreth, W., Fierstein, J., and Calvert, A. (2017). Early Postcaldera Rhyolite and Structural Resurgence at Long Valley Caldera, California. *J. Volcanology Geothermal Res.* 335, 1–34. doi:10.1016/j.jvolgeores.2017.01.005

Hippolyte, J. C., Angelier, J., and Roure, F. B. (1994). A Major Geodynamic Change Revealed by Quaternary Stress Patterns in the Southern Apennines (Italy). *Tectonophysics* 230 (3-4), 199–210. doi:10.1016/0040-1951(94)90135-x

Holohan, E. P., Troll, V. R., Walter, T. R., Münn, S., McDonnell, S., and Shipton, Z. K. (2005). Elliptical Calderas in Active Tectonic Settings: an Experimental Approach. *J. Volcanology Geothermal Res.* 144 (1-4), 119–136. doi:10.1016/j.jvolgeores.2004.11.020

Hurwitz, S., Christiansen, L. B., and Hsieh, P. A. (2007). Hydrothermal Fluid Flow and Deformation in Large Calderas: Inferences from Numerical Simulations. *J. Geophys. Res. Solid Earth* 112 (B2). doi:10.1029/2006jb004689

Kennedy, B. M., Mark Jellinek, A., and Stix, J. (2008). Coupled Caldera Subsidence and Stirring Inferred from Analogue Models. *Nat. Geosci* 1 (6), 385–389. doi:10.1038/ngeo206

Kennedy, B., Wilcock, J., and Stix, J. (2012). Caldera Resurgence during Magma Replenishment and Rejuvenation at Valles and Lake City Calderas. *Bull. Volcanol* 74 (8), 1833–1847. doi:10.1007/s00445-012-0641-x

L. Vezzoli (Editor) (1988). *Sland of Ischia, C.N.R. I* (Rome: Quaderni de "La Ricerca scientifica"), 114 135, 135.

Manzo, M., Ricciardi, G. P., Casu, F., Ventura, G., Zeni, G., Borgström, S., et al. (2006). Surface Deformation Analysis in the Ischia Island (Italy) Based on Spaceborne Radar Interferometry. *J. Volcanology Geothermal Res.* 151 (4), 399–416. doi:10.1016/j.jvolgeores.2005.09.010

Marianelli, P., Sbrana, A., and Proto, M. (2006). Magma Chamber of the Campi Flegrei Supervolcano at the Time of Eruption of the Campanian Ignimbrite. *Geol* 34, 937–940. doi:10.1130/g22807a.1

Marianelli, P., and Sbrana, A. (1998). Risultati di misure di standard di minerali e di vetri naturali in microanalisi a dispersione di energia. *Atti Soc. Tosc. Sci. Nat. Mem. Serie A*. 105, 57–63.

Marsh, B. D. (2000). "Magma chambers," in *Encyclopedia of Volcanoes*. Editor H. Sigurdsson (New York: Elsevier), 191–206.

Marsh, B. D. (1984). On the Mechanics of Caldera Resurgence. *J. Geophys. Res.* 89 (B10), 8245–8251. doi:10.1029/jb089ib10p08245

Nappi, R., Alessio, G., Gaudiosi, G., Nave, R., Marotta, E., Siniscalchi, V., et al. (2018). The 21 August 2017 Md 4.0 Casamicciola Earthquake: First Evidence of Coseismic Normal Surface Faulting at the Ischia Volcanic Island. *Seismol. Res. Lett.* 89, 1323–1334. doi:10.1785/0220180063

Nunziata, C., and Rapolla, A. (1987). A Gravity and Magnetic Study of the Volcanic Island of Ischia, Naples (Italy). *J. volcanology geothermal Res.* 31 (3-4), 333–344. doi:10.1016/0377-0273(87)90076-x

Orsi, G., Gallo, G., and Zanchi, A. (1991). Simple-shearing Block Resurgence in Caldera Depressions. A Model from Pantelleria and Ischia. *J. Volcanology Geothermal Res.* 47 (1-2), 1–11. doi:10.1016/0377-0273(91)90097-j

Paige, S. (1913). The Bearing of Progressive Increase of Viscosity during Intrusion on the Form of Laccoliths. *J. Geology.* 21, 541–549. doi:10.1086/622098

Paoletti, V., D'Antonio, M., and Rapolla, A. (2013). The Structural Setting of the Ischia Island (Phlegrean Volcanic District, Southern Italy): Inferences from Geophysics and Geochemistry. *J. Volcanology Geothermal Res.* 249, 155–173. doi:10.1016/j.jvolgeores.2012.10.002

Paoletti, V., Di Maio, R., Cella, F., Florio, G., Motschka, K., Roberti, N., et al. (2009). The Ischia Volcanic Island (Southern Italy): Inferences from Potential Field Data Interpretation. *J. Volcanology Geothermal Res.* 179 (1-2), 69–86. doi:10.1016/j.jvolgeores.2008.10.008

Passaro, S., De Alteriis, G., and Sacchi, M. (2016). Bathymetry of Ischia Island and its Offshore (Italy), Scale 1:50.000. *J. Maps* 12 (1), 152–159. doi:10.1080/17445647.2014.998302

Pelullo, C., Cirillo, G., Iovine, R. S., Arienzo, I., Aulinas, M., Pappalardo, L., et al. (2020). Geochemical and Sr-Nd Isotopic Features of the Zaro Volcanic Complex: Insights on the Magmatic Processes Triggering a Small-Scale Prehistoric Eruption at Ischia Island (South Italy). *Int. J. Earth Sci. (Geol Rundsch)* 109 (8), 2829–2849. doi:10.1007/s00531-020-01933-6

Piochi, M., Bruno, P. P., and De Astis, G. (2005). Relative Roles of Rifting Tectonics and Magma Ascent Processes: Inferences from Geophysical, Structural, Volcanological, and Geochemical Data for the Neapolitan Volcanic Region (Southern Italy). *Geochem. Geophys. Geosystems* 6 (7). doi:10.1029/2004gc000885

Piochil, M., Civetta, L., and Orsil, G. (1999). Mingling in the Magmatic System of Ischia (Italy) in the Past 5 Ka. *Mineralogy Pet.* 66, 227–258. doi:10.1007/bf01164495

Ricco, C., Alessio, G., Aquino, I., Brandi, G., Brunori, C. A., D'Errico, V., et al. (2019). High Precision Leveling Survey Following the Md 4.0 Casamicciola Earthquake of August 21, 2017 (Ischia, Southern Italy): Field Data and Preliminary Interpretation. *Ann. Geophys.* 61 (6), 665.

Rittmann, A. (1930). *Geologie der Insel Ischia. (Berlino) Zeitschrift für Vulkanologie*. (Berlin), VI, 268.

Rittmann, A., and Gottini, V. (1980). L'isola d'Ischia-Geologia. *Bollettino Del. Servizio Geologico Italiano* 101, 131–274.

Roedder, E. (1984). Fluid Inclusions. *Rev. Mineralogy* 12, 646. doi:10.1515/9781501508271

Sacchi, M., Pepe, F., Corradino, M., Insinga, D. D., Molisso, F., and Lubritto, C. (2014). The Neapolitan Yellow Tuff Caldera Offshore the Campi Flegrei: Stratal Architecture and Kinematic Reconstruction during the Last 15ky. *Mar. Geology.* 354, 15–33. doi:10.1016/j.margeo.2014.04.012

Sbrana, A., Biagio, G., Cubellis, E., Faccenna, C., Fedi, M., Fiorio, G., et al. (2011). *Carta Geologica della Regione Campania, scala 1:10000, Foglio 464 Isola di Ischia, Note Illustrative, aree emerse. Regione Campania, Assessorato Difesa del Suolo*. Firenze: LAC, 216.

Sbrana, A., Fulignati, P., Marianelli, P., Boyce, A. J., and Cecchetti, A. (2009). Exhumation of an Active Magmatic-Hydrothermal System in a Resurgent Caldera Environment: the Example of Ischia (Italy). *J. Geol. Soc.* 166, 1061–1073. doi:10.1144/0016-76492009-030

Sbrana, A., Marianelli, P., and Pasquini, G. (2021). The Phlegrean Fields Volcanological Evolution. *J. Maps*. doi:10.1080/17445647.2021.1982033

Sbrana, A., Marianelli, P., and Pasquini, G. (2018). Volcanology of Ischia (Italy). *J. Maps* 14 (2), 494–503. doi:10.1080/17445647.2018.1498811

Selva, J., Acocella, V., Bisson, M., Caliro, S., Costa, A., Della Seta, M., et al. (2019). Multiple Natural Hazards at Volcanic Islands: a Review for the Ischia Volcano (Italy). *J. Appl. Volcanology* 8 (1), 1–43. doi:10.1186/s13617-019-0086-4

Selva, J., Azzaro, R., Taroni, M., Tramelli, A., Alessio, G., Castellano, M., et al. (2021). The Seismicity of Ischia Island, Italy: an Integrated Earthquake Catalogue from 8th century BC to 2019 and its Statistical Properties. *Front. Earth Sci.* 9, 203. doi:10.3389/feart.2021.629736

Sepe, V., Atzori, S., and Ventura, G. (2007). Subsidence Due to Crack Closure and Depressurization of Hydrothermal Systems: a Case Study from Mt Epomeo (Ischia Island, Italy). *Terra Nova* 19 (2), 127–132. doi:10.1111/j.1365-3121.2006.00727.x

Servizio Geologico D'italia (2018). Geological Map of Italy, F 464 Isola d'Ischia. 1: 25000 – ISPRA Geological Survey of Italy, ISPRA Roma. Available at: https://www.isprambiente.gov.it/Media/carg/464_ISOLA_DISCHIA/Foglio.html.

Sibson, R. H. (1981). Controls on Low-Stress Hydro-Fracture Dilatancy in Thrust, Wrench and normal Fault Terrains. *Nature* 289 (5799), 665–667. doi:10.1038/289665a0

Silver, L. A., Ihinger, P. D., and Stolper, E. (1990). The Influence of Bulk Composition on the Speciation of Water in Silicate Glasses. *Contr. Mineral. Petrol.* 104, 142–162. doi:10.1007/bf00306439

Steinmann, L., Spiess, V., and Sacchi, M. (2018). Post-collapse Evolution of a Coastal Caldera System: Insights from a 3D Multichannel Seismic Survey from the Campi Flegrei Caldera (Italy). *J. Volcanology Geothermal Res.* 349, 83–98. doi:10.1016/j.jvolgeores.2017.09.023

Torrente, M. M., Milia, A., Bellucci, F., and Rolandi, G. (2010). Extensional Tectonics in the Campania Volcanic Zone (Eastern Tyrrhenian Sea, Italy): New Insights into the Relationship between Faulting and Ignimbrite Eruptions. *Ital. J. Geosciences* 129 (2), 297–315. doi:10.3301/ijg.2010.07

Trasatti, E., Acocella, V., Di Vito, M. A., Del Gaudio, C., Weber, G., Aquino, I., et al. (2019). Magma Degassing as a Source of Long-Term Seismicity at Volcanoes: The Ischia Island (Italy) Case. *Geophys. Res. Lett.* 46 (24), 14421–14429. doi:10.1029/2019gl085371

Vezzoli, L., Principe, C., Malfatti, J., Arrighi, S., Tanguy, J. C., and Le Goff, M. (2009). Modes and Times of Caldera Resurgence: The< 10 Ka Evolution of Ischia Caldera, Italy, from High-Precision Archaeomagnetic Dating. *J. Volcanology Geothermal Res.* 186 (3-4), 305–319. doi:10.1016/j.jvolgeores.2009.07.008

Wallace, P. J., Anderson, A. T., Jr., and Davis, A. M. (1999). Gradients in H2O, CO2, and Exsolved Gas in a Large-Volume Silicic Magma System: Interpreting the Record Preserved in Melt Inclusions from the Bishop Tuff. *J. Geophys. Res.* 104, 20097–20122. doi:10.1029/1999jb900207

Walter, T. R., and Troll, V. R. (2001). Formation of Caldera Periphery Faults: an Experimental Study. *Bull. Volcanology* 63 (2), 191–203. doi:10.1007/s004450100135

**Conflict of Interest:** The authors declare that the research was conducted in the absence of any commercial or financial relationships that could be construed as a potential conflict of interest.